A Study on Hybrid-Field Channel Estimation for E-MIMO in the Upper-Mid Band

Yekaterina Kim, Iqra Hameed, Hyunwoo Park, Nakyung Lee, Hanvit Kim, Sunwoo Kim

Department of Electronic Engineering, Hanyang University

{kattykimchi, iqrahameed, stark95, nagyeong2379, dante0813, remero}@hanyang.ac.kr

Abstract

The upper-mid band, a promising candidate for 6G, necessitates investigation of its frequency response to unlock the potential of extreme massive MIMO (E-MIMO). However, E-MIMO requires new approaches to channel estimation due to the hybrid-field nature of the channel, which combines near-field and far-field components. Given the limited research on hybrid-field channel estimation in the upper-mid band, this work investigates an orthogonal matching pursuit (OMP)-based method for E-MIMO channel estimation in this context. Simulation results highlight the need for further refinement in the accuracy and robustness of the proposed OMP-based method for E-MIMO channel estimation in the upper-mid band.

I. Introduction

The upper-mid band (7-24GHz) [1] offers better coverage than mmWave (above 24GHz) and higher data rates than sub-6GHz (below 6GHz). To satisfy 6G requirements on spectral efficiency and spatial resolution, extreme massive MIMO (E-MIMO) can be utilized. E-MIMO requires considering the near-field, characterized by spherical radial waves [2]. Due to several factors (e.g. the multipath effect), the E-MIMO channel combines far-field and near-field components, forming a hybrid-field channel, composed of components received from scatterers in both fields. While there has been research on hybrid-field channel estimation in mmWave [3]-[5], none has addressed the E-MIMO hybrid-field channel estimation in the upper-mid band. Therefore, this paper investigates methods for hybrid-field channel estimation in the upper-mid band.

II. System model

In this study, we employed the system model outlined in [3],[4]. The transmitting base station (BS) is equipped with a uniform linear array with N antennas spaced a half-wavelength apart $d = \lambda/2$, where λ is a wavelength. Single antenna user receives pilot signals from the BS during T time slots.

The received pilot signal is

$$\mathbf{r} = \mathbf{A}\mathbf{h} + \mathbf{n}, \tag{1}$$

where $\mathbf{h} \epsilon \mathbb{C}^{N\times 1}$ and $\mathbf{A} \in \mathbb{C}^{T\times N}$ denote the channel and transmitted pilot signal, $\mathbf{n} \sim CN(\mathbf{0}, \sigma^2\mathbf{I})$ represents received noise. $\mathbf{r} \epsilon \mathbb{C}^{T\times 1}$ and $\mathbf{A}$ are premised known.

The far-field channel $\boldsymbol{h}_{FF}$ can be expressed as follows [4]:

$$\boldsymbol{h}_{FF} = \sqrt{\frac{N}{P_{FF}}} \sum_{p=1}^{P_{FF}} g_p^{FF} \boldsymbol{a}(\theta_p), \tag{2}$$

where P_{FF} denotes the number of far-field scatterers,

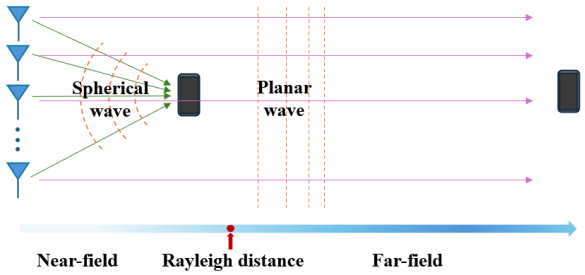

Fig.1. The near-field and far-field regions.

g_p^{FF} is the p^{th} far-field path's gain. The $\boldsymbol{a}(\theta_p)$ is the far-field array steering vector with $\theta_p = 2d\cos(\varphi_p)/\lambda$, where $\varphi_p \epsilon (0, \pi)$ is the physical angle:

$$\boldsymbol{a}(\theta_p) = \frac{1}{\sqrt{N}} \left[1, e^{-j\pi\theta_p}, \dots, e^{-j(N-1)\pi\theta_p}\right]^{\mathrm{H}}. \tag{3}$$

The channel can be represented using its sparse angular-domain representation $\boldsymbol{h}_{FF}^{A}$ as:

$$\boldsymbol{h}_{FF} = \mathbf{F}\boldsymbol{h}_{FF}^{A}, \tag{4}$$

where $\mathbf{F} = [\boldsymbol{a}(\theta_1), \dots, \boldsymbol{a}(\theta_N)]$ is the discrete Fourier transform matrix with N orthogonal steering vectors $\boldsymbol{a}(\theta_n)$ obtained by sampling the angular space by $\theta_n = (2n - N + 1)/N$, $n = 0, 1, \dots, N-1$ [3].

The near-field channel can be represented as [4]

$$\boldsymbol{h}_{NF} = \sqrt{\frac{N}{P_{NF}}} \sum_{p=1}^{P_{NF}} g_p^{NF} \boldsymbol{b}(\theta_p, r_p), \tag{5}$$

where the array steering vector

$$\boldsymbol{b}(\theta_p, r_p) = \frac{1}{\sqrt{N}} \left[1, e^{-j\frac{2\pi}{\lambda}\left(r_p^{(1)} - r_p\right)}, \dots, e^{-j\frac{2\pi}{\lambda}\left(r_p^{(N)} - r_p\right)}\right]^{\mathrm{H}}, \tag{6}$$

where g_p^{NF}, r_p denote the p^{th} near-field path's gain and the distance between the p^{th} near-field scatterer and the center of the antenna array. The distance between the n^{th} BS antenna and the p^{th} scatterer is denoted as $r_p^{(n)} = \sqrt{r_p^2 + \delta_n^2 d^2 - 2r_p\delta_n d\theta_p}$ and $\delta_n = (2n - N + 1)/2$.

The near-field channel $\boldsymbol{h}_{NF}$ can be represented via a polar-domain transform matrix $\mathbf{W}$ [3]:

$$\mathbf{W} = \left[\boldsymbol{b}(\theta_1, r_1^1), \ldots, \boldsymbol{b}\left(\theta_1, r_1^{S_1}\right), \ldots, \boldsymbol{b}(\theta_N, r_N^1), \ldots, \boldsymbol{b}\left(\theta_N, r_N^{S_N}\right)\right], \quad (7)$$

$$\boldsymbol{h}_{NF} = \mathbf{W}\boldsymbol{h}_{NF}^{P}, \quad (8)$$

where $\boldsymbol{h}_{NF}^{P}$ denotes the polar-domain channel and $s_n = 1,2,\ldots,S_N$ denotes the sampled distance index at the sampled angle θ_n.

III. Hybrid-field channel estimation method

The hybrid-field channel can be represented as [4]:

$$\boldsymbol{h}_{HF} = \sqrt{\frac{N}{P_{FF}}}\sum_{p=1}^{P_{FF}} g_p \boldsymbol{a}(\theta_p) + \sqrt{\frac{N}{P_{NF}}}\sum_{p=1}^{P_{NF}} g_p \boldsymbol{b}(\theta_p, r_p). \quad (9)$$

To address lacking sparsity in distance, the near-field component needs to be additionally sampled in distance at the sampled angle [3]. By employing equations (4) and (8), the hybrid-field channel can be represented as:

$$\boldsymbol{h}_{HF} = \boldsymbol{h}_{FF} + \boldsymbol{h}_{NF} = \mathbf{F}\boldsymbol{h}_{FF}^{A} + \mathbf{W}\boldsymbol{h}_{NF}^{P}. \quad (10)$$

The received signal is:

$$\mathbf{r} = \mathbf{A}\mathbf{F}\boldsymbol{h}_{FF}^{A} + \mathbf{A}\mathbf{W}\boldsymbol{h}_{NF}^{P} + \boldsymbol{n}. \quad (11)$$

This paper studied the method based on the orthogonal matching pursuit (OMP) algorithm for the hybrid-field channel estimation [4]. Support sets for each field are initialized empty. The sensing matrix of the estimated field is compared to the residual vector $\boldsymbol{v}$. The index of the most correlated column is updated as new support in the corresponding support set. The current path's channel is calculated using the least squares accordingly with the support set. As the path's channel component is estimated, $\boldsymbol{v}$ is reduced by the value of that component. Then, iteration starts over until the channel component $\widehat{\boldsymbol{h}}_{FF}$ or $\widehat{\boldsymbol{h}}_{NF}$ is estimated. The estimated hybrid-field channel $\widehat{\boldsymbol{h}}_{HF}$ is calculated as a sum of both fields' channel components with $\boldsymbol{v}$ updated by removing both field components if any exist.

IV. Simulation results

To analyze hybrid-field channel estimation for the E-MIMO system in the upper-mid band, we conducted a simulation considering frequencies $f = 30GHz$ and $f = 15GHz$, and a uniform linear antenna array with $N = 512$. The path gain g_p, angle θ_p and distance r_p were generated as $g_p \sim CN(0,1), \theta_p \sim U(-1,1), r_p \sim U(20,160)$ meters. The pilot signal is transmitted during $T = 256$ time slots. The number of paths is P. The minimum mean square error (MMSE) is used as a benchmark. The performance of the analyzed channel estimation scheme is evaluated in terms of the normalized mean square error (NMSE).

Fig. 2 shows the estimation performance for different ratios γ of near-field and far-field components in the hybrid field when $P = 12$. $\gamma = 0$ indicates a purely near-field channel, while $\gamma = 1$ represents a purely far-field channel. The performances are similar at both 15GHz and 30GHz, both outperforming MMSE. This shows that the method is applicable to both the upper-mid band and mmWave.

As shown in Fig. 3, this method provides satisfactory result for upper-mid band frequency when $P = 12$, even surpassing MMSE. However, in denser environments $P = 20, 24$ the method's performance degrades significantly.

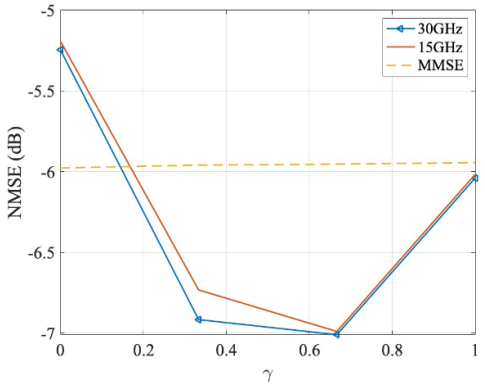

Fig.2 NMSE vs γ performance for f=15/30GHz

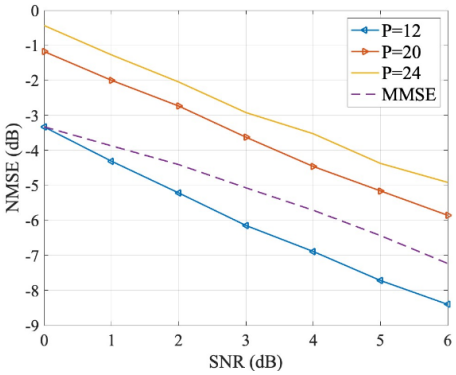

Fig.3 NMSE vs SNR performance for P=[12,20,24]

V. Conclusion

In this study, we demonstrated that the OMP-based hybrid-field channel estimation method for E-MIMO exhibits adequate performance in the upper-mid band in low-density environments. However, in the denser environments, alternative methods are needed. Also, a limitation of the analyzed method is the requirement of the exact number of paths to be known a priori, which can be challenging to achieve in practice.

ACKNOWLEDGMENT

This work was supported by Institute of information & communications Technology Planning & Evaluation (IITP) grant funded by the Korea government (MSIT) (No. RS-2024-00397216, Development of the Upper-mid Band Extreme massive MIMO (E-MIMO))

REFERENCES

[1] 3GPP, TR 38.820 V16.1.0, 2021.

[2] Wang, Z. "A Tutorial on Extremely Large-Scale MIMO for 6G: Fundamentals, Signal Processing, and Applications," *IEEE Commun. Surv. & Tut.*, 2024.

[3] Cui, M., "Channel Estimation for Extremely Large-Scale MIMO: Far-Field or Near-Field?" *IEEE T. Commun.*, 2022.

[4] Wei, X., "Channel Estimation for Extremely Large-Scale Massive MIMO: Far-Field, Near-Field, or Hybrid-Field?" *IEEE Commun. Lett.*, 2022.

[5] Hu, Z., "Hybrid-Field Channel Estimation for Extremely Large-Scale Massive MIMO System", *IEEE Commun. Lett.*, 2023.